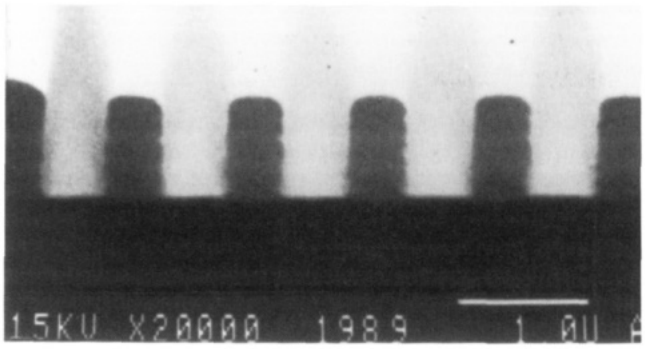

Figure 5. SEM micrograph depicting coded 0.5-μm images obtained in a 3:1 TBSS copolymer formulated with 5 wt % triphenylsulfonium hexafluoroarsenate.

T_g is that fully developed images may be treated at higher temperatures with no observed flow when TBSS is used as opposed to the parent styrene. The presence of up to 2% deprotection, as determined by NMR characterization, in TBSS did not affect the imaging characteristics of the system.

While some differences in resolution capability were observed for the materials described, it is not clear at this time whether the observed effects result from inherent materials characteristics or the lithographic process used to define the images. It does appear though, that sub-0.5-μm imaging is facilitated when the molecular weight of the copolymer is <300 000. A typical image that has been obtained in a TBSS resist system is depicted in Figure 5.

(21) Houlihan, F. M.; Neenan, T. X.; Reichmanis, E.; Kometani, J. M.; Chin, T. *Chem. Mater.* **1991**, *3*, 462.

Summary

TBSS is readily prepared via thermally induced free-radical bulk or solution polymerization. The copolymerization conditions, e.g., temperature and monomer concentration, determine copolymer composition and molecular weight. The polymerization mechanism is complex but may be explained by the rate equations proposed by Barb, Matsuda, and Cais. ^{13}C NMR spectra of selected TBSS copolymers indicate that the monomer triad sequence distribution is identical for copolymers of equivalent composition prepared by different synthetic routes. ^{13}C NMR analysis was also useful in determining the extent of deprotection of the *t*-BOC moieties in the TBSS copolymers during copolymerization. The thermal deprotection reaction in TBSS occurs at approximately the same temperature as the parent styrene polymer, though the incorporation of SO_2 substantially raises the glass transition temperature. The extent of *t*-BOC removal at a given dose decreases with increasing SO_2 content in the polymer. This was ascribed to differences in the catalytic chain length and diffusion distance of the photogenerated acid. The imaging characteristics, however, remain unaffected, presumably due to solubility differences of the polymers.

Acknowledgment. We thank M. Cheng, D. A. Mixon, F. M. Houlihan, T. X. Neenan, F. C. Schilling, A. E. Novembre, G. N. Taylor, and L. E. Stillwagon for technical assistance and many useful discussions concerning various aspects of this work.

Registry No. TBS, 87188-51-0; TBSS (copolymer), 120332-58-3; SO_2, 7446-09-5.

Synthesis and Characterization of a Catalytically Active Nickel–Silicoaluminophosphate Catalyst for the Conversion of Methanol to Ethene

J. M. Thomas,* Y. Xu, C. R. A. Catlow, and J. W. Couves

The Davy Faraday Research Laboratories, The Royal Institution, 21 Albemarle Street, London, W1X 4BS UK

Received January 22, 1991. Revised Manuscript Received May 15, 1991

X-ray absorption (near-edge and extended fine structure) along with diffuse reflectance infrared spectroscopy and other techniques are used to characterize specially prepared crystalline powdered samples of the title catalyst, which is based on the chabazite framework. It is established that the nickel ions that are all in tetrahedral, framework sites (first shell Ni–O distance lying close to 1.98 Å), and the loosely bound extraframework protons are thought to be the key components of the catalyst for the highly selective conversion of methanol to ethene.

Introduction

There is a class of heterogeneous catalysts in which essentially all the atoms of the bulk of the solid participate directly or are implicated indirectly in the key catalytic processes of the overall reaction. Well-known examples are zeolites, the silicoaluminophosphates (SAPOs), metal–aluminophosphates (MeAPOs), and also the various ion-exchanged sheet aluminosilicate clays such as montmorillonite and their pillared variants.[1,2] In such solid catalysts the "active sites" are distributed in a more or less spatially uniform fashion throughout the bulk of the solid. This means that they are amenable to characterization by most of the traditional and recently developed techniques

(1) Thomas, J. M. *Angew. Chem., Int. Ed. Engl.* **1988**, *27*, 1673.
(2) Thomas, J. M. *Philos. Trans. R. Soc. London, A* **1990**, *333*, 173.

0897-4756/91/2803-0667$02.50/0

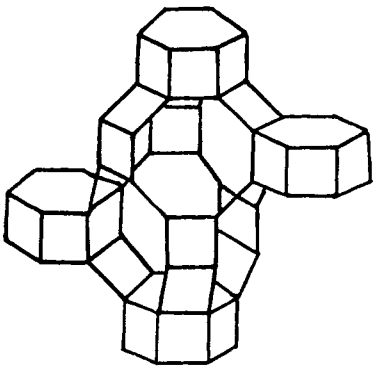

Figure 1. Representation of a segment of the framework of chabazite.

of solid-state chemistry and physics.

A specific heterogeneous catalyst that appears to fall into this category is that recently reported by Inui et al.[3] where nickel substitution into a silicoaluminophosphate results in highly selective conversion of methanol to ethene, a particularly important reaction in the context of maximizing yield of alkene as against that of liquid aromatic products, favored with the large-pore ZSM-5-based analogues.[4] What is so remarkable about this catalyst is the singular selectivity of the conversion of the methanol to ethene. Almost without exception all other zeolitic and aluminophosphate-based catalysts possessing an acidic character yield a range of numerous other products. Thus a broad range of hydrocarbons, encompassing C_2–C_4 alkenes, C_1–C_6 alkanes, and benzene, toluene, and xylenes, are produced (typically at 400 °C) from SAPO-5 and its zinc, manganese, cobalt, or germanium analogues (ZAPO-5, MnAPO-5, CoAPO-5, and GeAPO-5), whereas the weaker acid catalyst $ALPO_4$-5 and its titanium, boron, and iron analogues (TAPO-5, BAPO-5, and FAPO-5) all yield dimethyl ether.[5] Likewise the H^+ form of SAPO-34 efficiently converts methanol to a range of alkenes and alkanes.[6]

The particular framework structure of this new catalyst is known[3] to be of the "34" type, in the classification of Lok et al.[7-9] SAPO-34 has the same framework structure as that of the naturally occurring zeolite mineral chabazite (Figure 1). There is little doubt that in the H^+SAPO-34 catalyst one of the keys to the conversion is the loosely bound extraframework proton, which facilitates the production of intermediate carbocations and other transitory species. With the Ni–SAPO-34 catalyst of Inui et al. it is not clear whether all or some of the Ni^{2+} cations are in the framework of the SAPO and whether framework distortions as well as shape selectivity play a part in the catalysis. One of the major objectives of this investigation was to pinpoint the precise location of the Ni^{2+} ions in the active catalyst.

It has not yet proved possible to synthesize good-quality single crystals of the catalyst, but we have found a clean, effective method of preparing phase-pure powdered samples, which we have subjected to a range of investigations, as described below.

Experimental Section

Synthesis of nickel–SAPO-34 was achieved using a hydrothermal crystallization technique, which we have previously shown enables the preparation of highly crystalline metal-substituted $AlPO_4$-5[10] and Co–SAPO-34[11] the transition metal being, it is thought, in the aluminophosphate framework.

Ni–SAPO-34 was prepared by adding $NiCl_2{\cdot}6H_2O$ (guaranteed grade reagent from BDH chemicals) and SiO_2 Cabosil powder (guaranteed grade reagent Fluka Chemicals Ltd.) to a stirred aluminum phosphate solution, of P:Al:H_2O ratio of 1:0.6:50.[10] The organic templating agent, triethylamine (analytical grade from BDH) was slowly added and stirred vigorously for 5 h. Finally, F^- ions in the form of 40% hydrofluric acid (analytical grade reagent from BDH) was added to the gel mixture and stirred until a homogeneous solution, of final reaction composition

$$1.0P_2O_5{:}0.6Al_2O_3{:}0.2SiO_2{:}(0.01\text{–}0.03)Ni^{2+}{:}(2.6\text{–}4.5)Et_3N{:}(40\text{–}100)H_2O{:}(0.2\text{–}1.0)F^-$$

was obtained. The gel mixture was transferred to a PFTE-lined stainless steel autoclave. Crystallization was performed at 200 °C for 36 h. The product was isolated by filtration, washed with boiling water, and dried at 110 °C overnight. The Ni–SAPO-34 was then calcined at 550 °C in air for 3 h.

Chemical analysis was kindly performed at Kingston Polytechnic using inductively coupled plasma (ICP) spectroscopy. Simultaneous thermogravimetric and differential thermal analysis were recorded on a Stanton-Redcroft (STA-1500) system. Approximately 10 mg of sample was heated at 10 °C/min under flowing dry nitrogen. X-ray powder diffraction studies were performed on a Siemens D500 powder diffractometer with DIFFRAC 500 software, using Cu Kα radiation with a graphite single-crystal secondary monochromator.

Extended X-ray absorption fine structure (EXAFS) data were collected at the Synchrotron Radiation Source of the SERC Daresbury Laboratory. The data, acquired on station 7.1 with an electron energy of 2 GeV and ring current 200–140 mA, were collected with a Si(111) double-crystal monochromator at the Ni K edge (8332 eV). EXAFS data processing was performed using the Daresbury Laboratory EXAFS analysis suit of programs EXCALIB, EXBACK, and EXCURV90.[12] Nickel oxide was used to determine nickel oxygen phase-shift corrections; calculated phase shifts were used for phosphorus and carbon. All spectra were fitted in the K-space range 4–12 $Å^{-1}$ by using curved-wave approximations.

EXAFS spectra were recorded for $NiCr_2O_4$ and five different samples of the Ni–SAPO-34. The latter was used as-prepared, with triethylamine template (Ni–SAPO34A) and a calcined (detemplated) sample (Ni–SAPO34B). EXAFS spectra were also recorded on samples of the calcined material that under catalytic conditions (250 °C in methanol/nitrogen) produced nearly 100% ethene selectivity (Ni–SAPO34C) and a sample that under different catalytic conditions (400 °C in methanol/nitrogen) showed poor selectivity to methanol (Ni–SAPO34D). Finally the EXAFS of a lithium ion exchanged Ni–SAPO34 was studied.

The testing of Ni–SAPO-34 catalyst in the conversion of methanol to olefins was carried out in a flow reaction system under the following conditions: 200-mg samples of catalyst were activated at 400 °C overnight. Methanol (0.2 atm) was carried into the reaction bed by flowing nitrogen of balance pressure (0.8 atm). Activity was tested in the temperature range 200–450 °C, using a fresh catalyst sample for each temperature. Product gases were analyzed with a Perkin-Elmer gas chromatograph, with flame ionization detector, using a Chrom-P column to separate C_1–C_5 hydrocarbons, after 2 h on line and monitored for a further 4 h. Retention times and response factors were determined by using

(3) Inui, T., Phatanasri, S.; Mutsuda, H. *J. Chem. Soc., Chem. Commun.* **1990**, 205.
(4) Chang, C. D. *Catal. Rev. Sci.* **1980**, *112*, 11.
(5) Ione, K. G.; Kihetyanin, O. V.; Mastikhin, V. M. In *New Developments in Zeolite Science and Technology*; preprint of Poster papers of the 7th International Conference, Tokyo, Aug 1986; Japan association of Zeolite; Paper 3d-18, pp 325.
(6) Xu, Y.; Grey, C. P.; Thomas, J. M.; Cheetham, A. K. *Catal. Lett.* **1990**, *4*, 251.
(7) Wilson, S. T.; Lok, B. M.; Flanigen, E. M. US Patent 4,310,440, 1982.
(8) Messina, C. A.; Lok, B. M.; Flanigen, E. M. US Patent 4,544,143, 1985.
(9) Lok, B. M.; Messina, C. A.; Patton, R. L.; Gajek, R. T.; Cannan, T. R.; Flanigen, E. M. *J. Am. Chem. Soc.* **1984**, *106*, 6092.
(10) Xu, Y.; Maddox, P. J.; Thomas, J. M. *Polyhedron* **1989**, *8*, 819.
(11) Xu, Y.; Maddox, P. J.; Couves, J. W. *J. Chem. Soc., Faraday Trans.* **1990**, *86*, 425.
(12) Binstead, N.; Gurman, S. J.; Ross, I. *J. Phys. C* **1984**, *17*, 143; SERC Daresbury Laboratory Update, 1990.

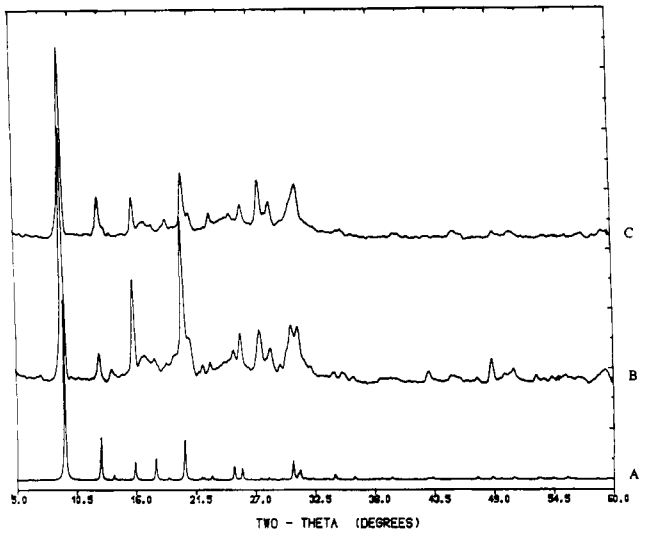

Figure 2. (A) Simulated X-ray powder diffraction pattern of the protonated form of SAPO-34 from Ito et al.[12] (B) X-ray powder diffraction pattern of as-prepared Ni-SAPO-34. (C) X-ray powder diffraction pattern of Ni-SAPO-34 after in situ calcination at 550 °C (y axis counts/s).

a standard gas mixture calibration.

Diffuse reflectance infrared Fourier transform spectra (DRIFTS) were recorded on a Perkin-Elmer 1725X FTIR spectrometer fitted with a Spectratech diffuse reflectance attachment. Samples of H-SAPO-34 and Ni-SAPO-34 were calcined at 550 °C for 15 h in a stream of dry air by using a Spectratech diffuse reflectance environmental cell.

Results and Discussion

The chemical formulas of the Ni-SAPO-34 derived from inductively coupled plasma was $[P_{12.7}Si_{5.4}Al_{17.6}Ni_{0.3}O_{72}]$, which means that there is an overall negative charge (5.5 per unit cell) on the framework. The tetrahedral sites of $ALPO_4$s are occupied alternately by aluminum and phosphorus, so the idealized formulas for the pure $ALPO_4$-34 is $[P_{18}Al_{18}O_{72}]$. In SAPO-34, as with other SAPOs, silicon preferentially substitutes on the phosphorus site.[11,13] There is only a small degree of nickel substitution on the aluminum site (Al/Ni = 58.7). The chemical analysis also suggests that there are no extraframework nickel cations present, in contrast to the situation obtained for the cobalt analogue.[11] The framework negative charge is thus compensated for solely by protons, which are available for acid catalysis.

X-ray powder diffraction studies of the as-prepared material (Figure 2) indicate a crystalline material consistent with the simulated diffraction pattern of chabazite derived from the coordinates of Ito et al.[14] Heating Ni-SAPO-34 to 550 °C for 4 h (Figure 2) results in a material that retains the integrity of the chabazite structure. Such changes as occur in the intensity of the *hkl* reflections are a result of the loss of the triethylamine, which is accompanied by a slight expansion of the lattice.

The differential thermal analysis data are shown in Figure 3. The low-temperature endotherm is associated with loss of water between 85 and 114 °C. These are followed by thermal activity at 395, 403, and 456 °C, which are assignable to loss of occluded template. The loss of template from the metal-substituted SAPO-34 is significantly more complicated than that of SAPO-34 itself owing to local electronic variations within the channel. This has

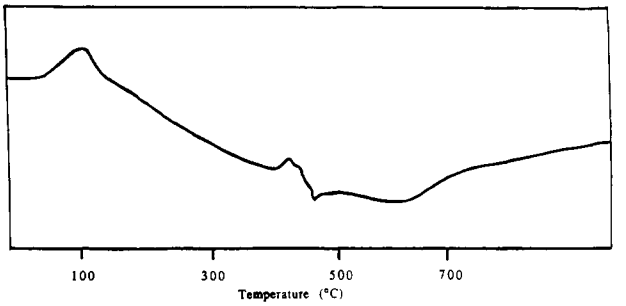

Figure 3. Differential thermal analysis of as-prepared Ni-SAPO-34 in nitrogen (*Y* axis dc output).

Table I. Effect of Temperature on the Product Distribution of Methanol Conversion over Ni-SAPO34, Recorded after 2 h On-Line

		selectivity,[a] %		
temp, °C	methanol conv, %	C_2H_4	CH_4	CO_2
250	90.5	94.5	0.5	0.6
300	92.7	84.3	3.9	3.6
350	95.4	81.6	5.8	4.7
400	96.4	72.1	8.9	6.6
450	95.3	60.5	12.3	8.7

[a] Trace amounts of ethane, propane, and propene were also observed in the effluent gas stream.

previously been noted for Co-$ALPO_4$-5[10] and Co-SAPO34.[11] The template is released at three distinct temperatures that correspond to loss of free amine and the degradation of the proton or metal amine complexes at a higher temperature. Dehydroxylation occurs at 613 °C and is associated with a 2.5% loss of weight. The structure was not observed to collapse in the temperature range studied. Ni-SAPO-34 is thus considerably more stable than Co-SAPO-34, for which structure collapse to a dense phase occurs at 680–700 °C.[11] This should be a consequence of the lower level of metal ion substitution in the framework.

Table I shows the results of the catalytic tests obtained for Ni-SAPO-34 in the methanol conversion reaction. Methanol was converted to ethene at 250 °C with nearly 100% selectivity and 90% conversion, no dimethyl ether being detected in the effluent gas stream. With increasing temperature there is only a slight increase in methanol conversion. However, the selectivity toward ethene decreases dramatically. Carbon dioxide, propene, and propane are detected at these higher temperatures. Compared to the H-SAPO-34,[6,15] the calcined Ni-SAPO-34 shows much greater selectivity to ethene. H-SAPO-34 converts methanol to light olefins, with an ethene selectivity of around 30%.

It is evident that the presence of nickel cations within the SAPO-34 structure has greatly increased its catalytic performance and selectivity toward ethene. X-ray diffraction studies reveal that the material still retains the chabazite framework. However, it is not possible, by X-ray powder diffraction, definitively to show the isomorphous substitution of Al^{3+} at the tetrahedral site by Ni^{2+}.

Nickel oxide was used as a standard for an octahedral oxygen environment around the transition-metal ion and nickel chromium oxide ($NiCr_2O_4$)[16] for nickel in a tetrahedral oxygen environment. Figure 4 shows the X-ray absorption spectra of NiO and $NiCr_2O_4$. $NiCr_2O_4$ has a significant preedge feature due to the 1s → 3d transition

(13) Manters, J. A.; Janseens, C.; Gorbet, P. J., Beyer, H. H.; Jacobs, P. A. *Stud. Surf. Sci. Catal.* **1989**, *49A*, 215.

(14) Ito, M.; Shimoyama, Y.; Saito, Y. *Acta. Crystallogr. C* **1985**, *4*, 1698.

(15) Liang, J.; Zhao, S. Q.; Li, H. Y.; Guo, W. G.; Ying, M. L. In *Extended Abstracts of an International Symposium on Zeolites as Catalysts, Sorbents and Detergents Builders*; International Zeolite Association: Wurzburg, 1988; p 59.

(16) Thomassen, L. *J. Am. Chem. Soc.* **1940**, *62*, 1134.

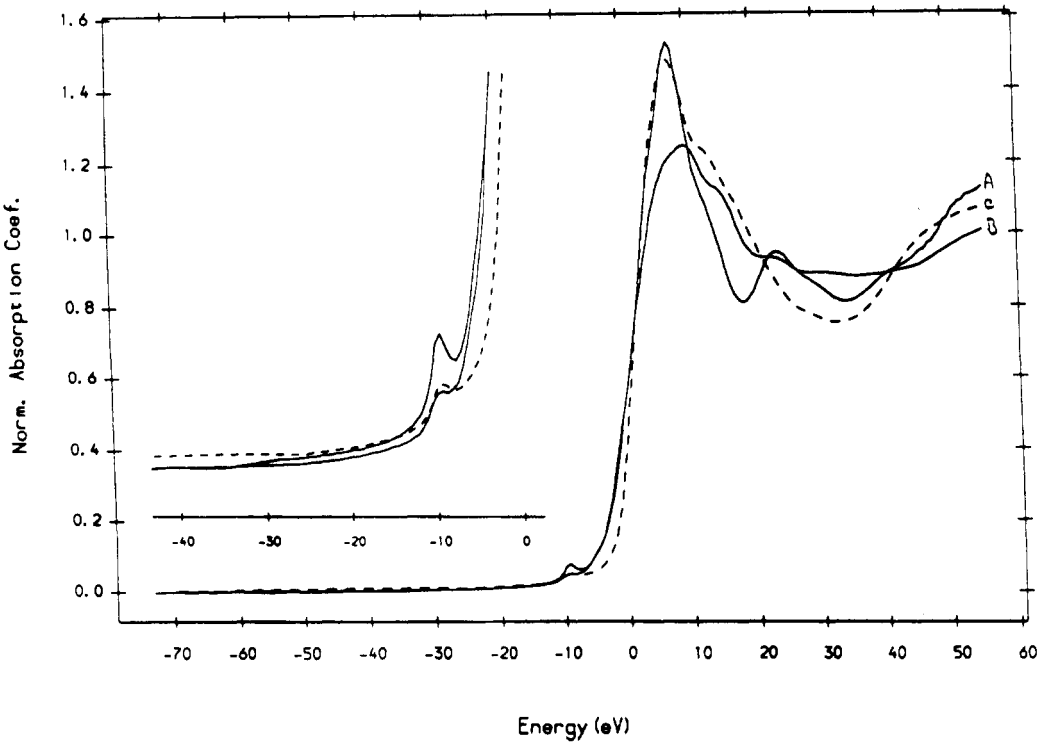

Figure 4. XANES region of the X-ray absorption spectra of (A) NiO, (B) $NiCr_2O_4$, and (C) Ni-SAPO-34A.

Table II. Coordination Numbers and Shell Distances Used in Curve Fitting of EXAFS Data

	first shell			second shell			third shell		
sample	R, Å	N^a	A^b	R, Å	N^a	A^b	R, Å	N^a	A^b
NiO	2.09	6 (O)	0.012	2.95	12 (Ni)	0.015			
NiCr2O4	1.94	4 (O)	0.017	3.34	8 (Cr)	0.017	3.65	8 (O)	0.039
Ni-SAPO34A	1.99	4.6 (O)	0.013	2.75	1.1 (O)	0.021	3.18	4.3 (P)	0.035
Ni-SAPO34B	1.99	4.4 (O)	0.012	2.69	1.5 (O)	0.019	3.17	3.8 (P)	0.033
Ni-SAPO34C	1.99	4.4 (O)	0.014	2.74	2.3 (O)	0.029	3.14	3.6 (P)	0.029
Ni-SAPO34D	1.98	4.3 (O)	0.014	2.73	2.4 (O)	0.026	3.13	4.3 (P)	0.040
Li-Ni-SAPO34	1.97	4.2 (O)	0.013	2.74	2.1 (O)	0.023	3.15	4.2 (P)	0.041

[a] Coordination number with backscattering atom in brackets. [b] A: Debye-Waller factor.

becoming allowed in the tetrahedral geometry, a result of s → p mixing. This preedge feature is significantly smaller in the case of nickel oxide (mixing of the O_{2p} and Ni_{3d} orbitals results in some p-orbital character, giving rise to the small preedge feature in nickel oxide). The X-ray absorption spectra of the Ni-SAPO-34 samples show a preedge feature intermediate between the two extremes, an indication that there is either a mixture of the two nickel environments or tetrahedral coordination with a lengthening of the Ni-O bond length, which reduces the probability of the 1s → 3d transition.

Curve-fitting of the extended X-ray absorption fine structure data derived from the X-ray absorption spectra of NiO and $NiCr_2O_4$ yielded values of phase shift corrections that were incorporated into the processing of the data from the catalyst samples. Figure 5 shows the fitted K^3-weighted EXAFS data. Table II summarizes the coordination number and bond distances used to fit the data. For both the more and less selective samples of the catalysts studied here, the first shell distance varies between 1.98 and 1.99 Å, significantly smaller than the 2.08 Å expected for octahedral nickel oxygen. This value is similar to the nickel–oxygen contact distance of 1.96 Å in the tetrahedral environment within $NiCr_2O_4$. The slight elongation is consistent with the decreased magnitude of the observed preedge feature. The first shell is best fitted to around 4.5 oxygen atoms in each case, broadly consistent with the tetrahedral geometry. The third shell can be fitted on the basis of approximately four P atoms at a distance of 3.15 Å. Assuming a P–O bond length of 1.54 Å, the bond angle around the O atom is thus estimated to be 128° in contrast to the value of 148° for the Al–O–P atom angle in SAPO-34[14] itself.

The first and third shells distances (Table II) are thus consistent with framework-substituted nickel causing a large perturbation of the local environment. However, there is a second intermediate shell present in each of the Ni-SAPO-34 samples studied. This fits to approximately 1 backscattering atom in the as-prepared material and around 2 backscattering atoms for the calcined samples. In all cases oxygen was assumed to be the backscattering atom. This may be an indication of the presence of hydrogen-bound water molecules within the coordination sphere.

There is little difference between the EXAFS data recorded for the calcined sample and those obtained on the samples after catalysis (Ni-SAPO34C and Ni-SAPO34D of Table II). This is taken to signify that no irreversible changes occur in the nickel environment during catalysis, although such a conclusion must be regarded as tentative until in situ X-ray absorption spectra are recorded during catalysis at elevated temperatures. The similarity of the EXAFS data for samples Ni-SAPO34C and Ni-SAPO34D is an indication that the diminished selectivity of the latter sample toward ethene formation is not primarily due to changes in the overall structure but is related to some

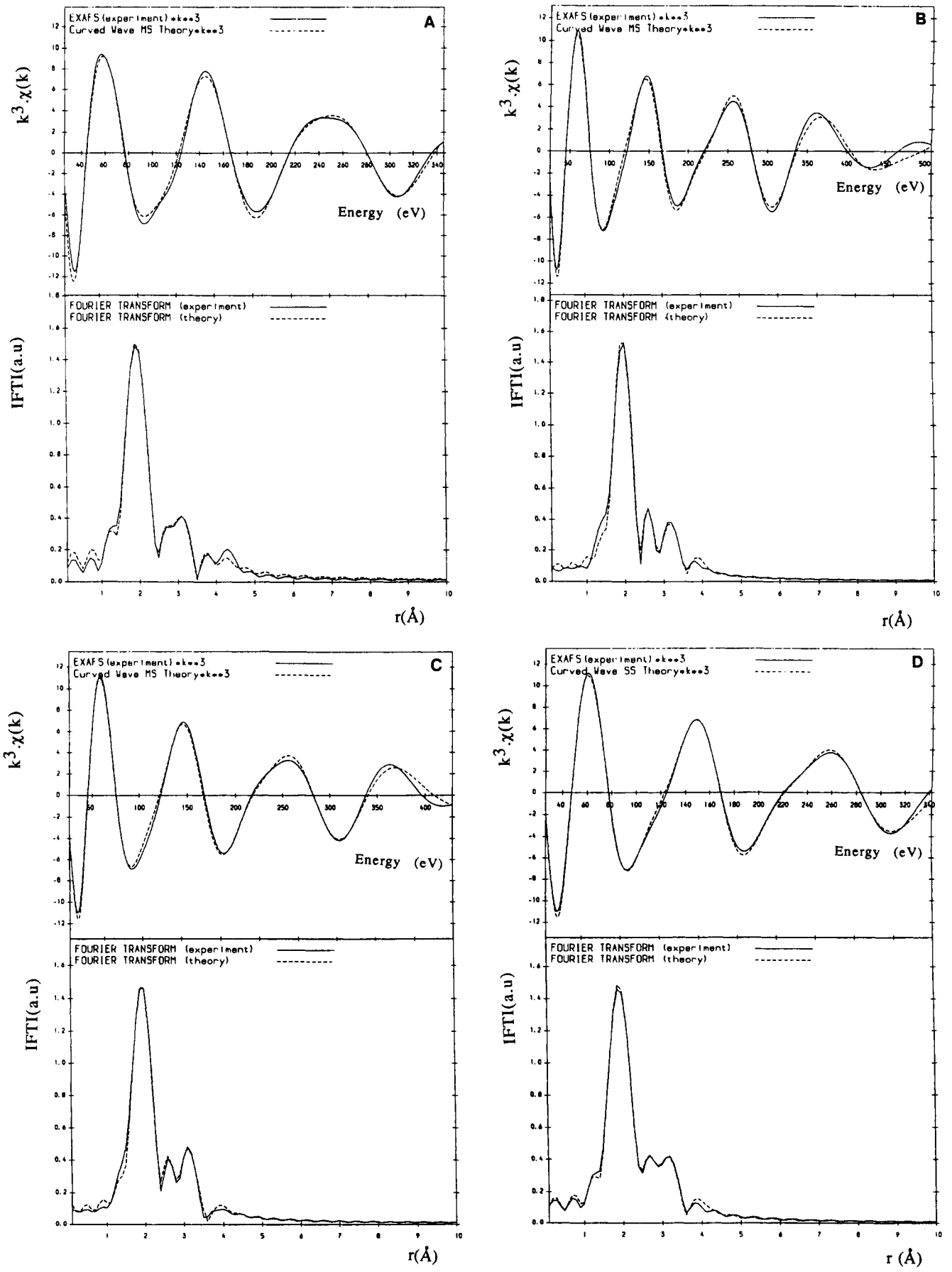

Figure 5. Fitted EXAFS data of Ni-SAPO-34A to Ni-SAPO-34D.

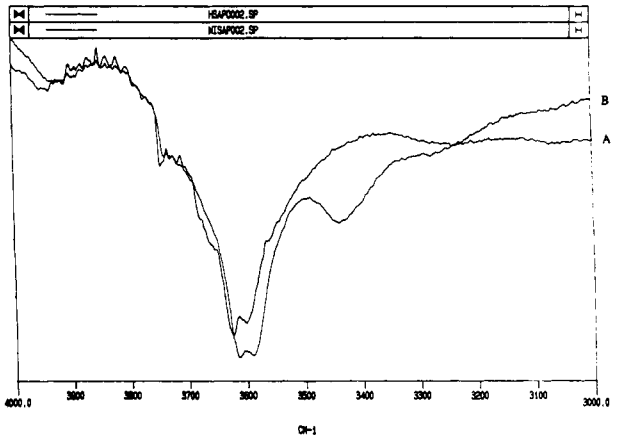

Figure 6. DRIFTS spectra of (A) calcined H-SAPO-34 and (B) Ni-SAPO-34.

subtleties of the mechanism of the catalytic reactions, doubtless arising from minor structural modifications of the active site. Finally, since the Li-NiSAPO34 again gave a similar EXAFS spectrum to that of the calcined Ni-SAPO34, this strongly indicates that the nickel cations cannot be present as exchangeable cations.

Diffuse reflectance infrared Fourier transform spectroscopy of calcined Ni-SAPO-34 shows the presence of a broad O-H stretching absorption band between 3490 and 3370 cm^{-1}, which is absent in the calcined SAPO-34 (Figure 6). We believe that this feature as well as the peaks at 3623 and 3597 cm^{-1} may be associated with Si-O(H)-Al Bronsted sites. Halik et al.[17] have assigned peaks close to 3623 and 3597 cm^{-1} to Bronsted acid sites of this kind in samples of SAPO similar to those used here. We are less clear of the origin of the broad peak centered around 3430 cm^{-1}. Adsorption of methanol at room temperature does not alter the broad feature. It is possible that there is a bridging hydrogen-bonded species present, which stabilizes the framework substitution of Ni in SAPO-34.

Since the O-H stretching bands of Ni-SAPO-34 are more intense than those of the H^+-SAPO-34, we conclude that the nickel-bearing catalyst has a higher density of acid sites. Its catalytic activity and selectivity is thus seen to be associated with the modification of the acidity of the zeolite by nickel and doubtless by subtle structural changes within the active site.

EXAFS analysis proves that the nickel is incorporated into the structure, with a large perturbation of the local environment. It also suggests the presence of a second extraframework coordination sphere, which from infrared spectroscopy seems to involve hydrogen bonding. This is postulated to stabilize the local structure around the nickel. We have, at present, no clear-cut evidence for the nickel having any direct role in the methanol conversion reaction, but it seems to modify the Bronsted acidity of the SAPO-34. Access to the nickel may be blocked by the bridging species observed by EXAFS and DRIFTS. Further investigations into the nature of the active site of this remarkable catalyst are underway.

Acknowledgment. We thank the Science and Engineering Research Council for its support and the British Council for a maintenance grant to Y.X. We also acknowledge the guidance and cooperation of Prof. G. N. Greaves and his colleagues at the SERC Daresbury Laboratory.

(17) Halik, C.; Lercher, J. A.; Meyer, H. *J. Chem. Soc., Faraday Trans. 1* **1988**, *84*, 4457.

Two Electronically Distinct Copper Sites in $La_{2-x}Sr_xCuO_{4-\delta}$ Compounds for $0.10 \leq x \leq 0.20$

Mark A. Kennard,[†,§] Yiqiao Song,[‡,§] Kenneth R. Poeppelmeier,[†,§,⊥] and W. P. Halperin*[,‡,§,⊥]

Department of Chemistry, Department of Physics and Astronomy, Materials Research Center, Science and Technology Center for Superconductivity, Northwestern University, Evanston, Illinois 60208

Received February 11, 1991. Revised Manuscript Received April 19, 1991

We report copper NQR and NMR measurements performed on the series $La_{2-x}Sr_xCuO_4$ ($0.10 \leq x \leq 0.20$). For each composition, two distinct sites of copper were observed. The relative occupation of the two sites correlates well with strontium doping. Transverse NMR shifts ($H \perp c$) of the two copper sites were derived from the NMR and NQR spectra. The temperature dependence of the ^{63}Cu NMR frequency shifts are identical for both sites, indicating that they have the same electronic spin susceptibility and hyperfine fields, and both are in the superconducting phase having the same critical temperature. However, these two sites have distinct orbital frequency shifts and electric field gradients.

Introduction

$La_{2-x}Sr_xCuO_{4-\delta}$ materials are structurally simpler than the other copper oxide superconductors. At room temperature, the superconducting members of this family have the tetragonal K_2NiF_4 structure space group $I4/mmm$-D_{4h}^{17} (ref 1) (see Figure 1) but convert to the orthorhombic structure $Abma$-D_{2h}^{18} (ref 2) by tilting of the oxygen octahedra below a transition temperature T_d. In both the

† Department of Chemistry.
‡ Department of Physics and Astronomy.
§ Materials Research Center.
⊥ Science and Technology Center for Superconductivity.

(1) Nguyen, N.; Choisnet, J.; Hervieu, M.; Raveau, B. *J. Solid State Chem.* **1981**, *39*, 120-127.
(2) Grande, V. B.; Müller-Buschbaum, Hk.; Schweizer, M. *Z. Anorg Allg. Chem.* **1977**, *428*, 120-124. Fleming, R. M.; Batlogg, B.; Cava, R. J.; Rietman, E. A. *Phys. Rev. B* **1987**, *35*, 7191.

0897-4756/91/2803-0672$02.50/0